



# HOKKAIDO UNIVERSITY

Title	Intra-annual variations in atmospheric dust and tritium in the North Pacific region detected from an ice core from Mount Wrangell, Alaska
Author(s)	Yasunari, Teppei J.; Shiraiwa, Takayuki; Kanamori, Syosaku et al.
Citation	Journal of Geophysical Research, 112(D10), D10208 <a href="https://doi.org/10.1029/2006JD008121">https://doi.org/10.1029/2006JD008121</a>
Issue Date	2007-05-19
Doc URL	<a href="https://hdl.handle.net/2115/26404">https://hdl.handle.net/2115/26404</a>
Rights	An edited version of this paper was published by AGU. Copyright 2007, American Geophysical Union, JOURNAL OF GEOPHYSICAL RESEARCH-ATMOSPHERES, 112.
Type	journal article
File Information	JGR-A112-D10.pdf



# Intra-annual variations in atmospheric dust and tritium in the North Pacific region detected from an ice core from Mount Wrangell, Alaska

Teppei J. Yasunari<sup>1</sup>, Takayuki Shiraiwa<sup>2</sup>, Syosaku Kanamori<sup>1</sup>, Yoshiyuki Fujii<sup>3</sup>, Makoto Igarashi<sup>4</sup>, Koji Yamazaki<sup>1</sup>, Carl S. Benson<sup>5</sup>, and Takeo Hondoh<sup>6</sup>

<sup>1</sup>Graduate School of Environmental Science, Hokkaido University, Kita-10, Nishi-5, Sapporo 060-0810, Japan. (tepei@hms.lowtem.hokudai.ac.jp; kanasyo@pop.lowtem.hokudai.ac.jp; yamazaki@ees.hokudai.ac.jp)

<sup>2</sup>Research Institute for Humanity and Nature, Motoyama 457-4, Kamigamo, Kita-ku, Kyoto 603-8047, Japan. (shiraiwa@chikyu.ac.jp)

<sup>3</sup>National Institute of Polar Research, Kaga 1-9-10, Itabashi-ku, Tokyo 173-8515, Japan. (fujii@pmg.nipr.ac.jp)

<sup>4</sup>RIKEN Wako Institute, 2-1, Hirosawa, Wako, Saitama 351-0198, Japan. (m-igarashi@riken.jp)

<sup>5</sup>Geophysical Institute, University of Alaska Fairbanks, Fairbanks, Alaska 99775-7320, USA. (benson@gi.alaska.edu)

<sup>6</sup>Institute of Low Temperature Science, Hokkaido University, Kita-19, Nishi-8, Sapporo 060-0819, Japan. (hnd@lowtem.hokudai.ac.jp)

## Abstract

The North Pacific is subject to various seasonal climate phenomena and material circulations. Therefore, intra-annual ice-core data is necessary for an assessment of the climate variations. To assess past variations, a 50-m ice core was drilled at the summit of the Mount Wrangell Volcano, Alaska. The dust number, tritium concentrations, and stable hydrogen isotope were analyzed. The period covered was from 1992 to 2002. We found that the concentrations of both fine dust (0.52–1.00  $\mu\text{m}$ ), an indicator of long-range transport, and coarse dust (1.00–8.00  $\mu\text{m}$ ) increased together every spring. Moreover, their concentrations increased drastically after 2000, corresponding to the recent increase in Asian dust outbreaks in spring. Additionally, an increase in the spring of 2001 corresponded to the largest dust storm recorded in East Asia since 1979. Therefore, our findings imply that Asian dust strongly polluted Mount Wrangell every spring. The stratospheric tracer, tritium, had late spring maxima almost every year and we found this useful for ice-core dating to identify late spring in the North Pacific region. We also found that a high positive-annual correlation existed between the calculated tritium and fine dust fluxes from late spring to summer. We propose that an annual relationship between the stratosphere-troposphere exchange and Asian dust storm are most closely connected in late spring because their activities are weak in summer. The Mount Wrangell ice core is important and useful for assessing the dust and tritium circulation in the distant past around the North Pacific with probable intra-annual time scale information.

Index Term: 0724 Ice cores (4932); 0305 Aerosols and particles (0345, 4801, 4906); 3362

Stratosphere/troposphere interactions; 0368 Troposphere: constituent transport and chemistry; 0720

Glaciers

## 1. Introduction

The North Pacific region is known to exhibit various climate phenomena such as the Pacific Decadal Oscillation (PDO) [Mantua *et al.*, 1997], El Niño-Southern Oscillation (ENSO) [Bjerknes, 1969], and Arctic Oscillation (AO) [Thompson and Wallace, 1998]. Therefore, a lot of geoscientists focus on this region and carry out research on subjects associated with these climate phenomena.

Ice-core study is one of the important fields for the reconstruction of historical climate changes in the North Pacific region. In the northern hemisphere, various ice cores were drilled mainly in the Atlantic section at locations such as Greenland and mountain glaciers [e.g., Thompson *et al.*, 2000; North Greenland Ice Core Project members, 2004]. In the North Pacific section, however, only few ice cores have been drilled so far. The locations are Mount Logan [Holdsworth *et al.*, 1992; Shiraiwa *et al.*, 2003], Eclipse ice field [Wake *et al.*, 2002] in the Yukon Territory, Canada, Mount Bona Churchill by L. G. Thompson, Mount Ushkovsky in Kamchatka, Russia [Shiraiwa *et al.*, 2001], and Mount Wrangell in the Saint Elias Range, Alaska [Shiraiwa *et al.*, 2004].

We particularly focus on the dust concentration in the Mount Wrangell ice core because it is known to have been associated with a large dust outbreak in the Asian continent in the North Pacific section. The atmospheric dust outbreaks in the northern hemisphere are mainly associated with dust storms [Iwasaka *et al.*, 1983], particularly storms in the Gobi and Taklamakan deserts of East Asia. The outbreak frequency is highest in March, April, and May, and the dust outbreak frequency has particularly increased after the year 2000 [Japan Meteorological Agency (JMA), 2004; Chun and

*Lim*, 2004]. The transport of Asian dust to Alaska was first identified in 1977 from aircraft samples [*Rahn et al.*, 1977] and it was also observed recently by elemental analysis using trajectory analysis [*Cahill*, 2003] and satellite observations [*Darmenova et al.*, 2005]. Hence, Asian dust has had impacts on Alaska for a long time.

In June 2003, a 50-m ice core was recovered from the summit of Mount Wrangell—a volcano located at 62°N, 144°W and 4100 m above sea level (a.s.l.) in Alaska [*Shiraiwa et al.*, 2004]. Mount Wrangell is an ideal site for ice-core study because of its proximity to the North Pacific, its high snow accumulation rate (1.3 m yr<sup>-1</sup> in water equivalent near the North Crater [*Benson and Motyka*, 1978]), and the relatively flat glacier surface (Figure 1). Consequently, an ice core with few melt-frozen layers was obtained. The summit is in the free troposphere and its surface is strongly affected by a westerly jet. Since insoluble microparticles (dust) are transported from East Asia to the summit of Mount Wrangell by this jet, the summit is probably the best site to detect the Asian dust. Therefore, the ice core drilled at the summit of Mount Wrangell can be ideal for investigating the past seasonal variations of dust from East Eurasia to Alaska around the North Pacific region.

In this work, we have analyzed the ice core drilled by *Shiraiwa et al.* [2004] and have successfully obtained various datasets of Mount Wrangell through seasonal dating. The other ice cores drilled in the region were drilled at sites with considerably lesser snow accumulations, and it was unfortunately difficult to discuss the seasonal events. The goal of an ice-core study is generally to reconstruct long-term information of the past atmospheric behavior extending beyond

contemporary meteorological observations. However, climate phenomena may vary on intra-annual time-scales. Therefore, a seasonal dataset of ice cores and their examination for seasonal variations of climate are necessary. If we could accurately discuss the details of seasonal climate variations from ice cores using many meteorological datasets that are available, then we could understand the distant past. It will also be helpful to simulate the past climate by General Circulation Model (GCM) studies in the future. In this study, we discuss important seasonal ice-core data in the North Pacific region.

## 2. Method

### 2.1. Ice core and snow sample analyses

The ice core was cut at intervals of 5–10 cm (some sections were slightly less than 5 cm) for a total of 643 samples for dust analysis, which corresponded to 31–143 samples per year and to roughly 3–12 days resolution. After cutting, we removed the surface of the samples to an extent of approximately 5 mm with a ceramic knife to remove the external contamination; this was done with clean-room clothes and poly gloves on a clean bench in a low-temperature clean room in a manner similar to that of *Fujii et al.* [2003]. The 50-m ice core was analyzed over its entire length for the dust particle number concentration in each range (0.52–0.71, 0.71–1.00, 1.00–1.42, 1.42–2.00, 2.00–2.82, 2.82–4.00, 4.00–5.70, 5.70–8.00, 8.00–11.15, and 11.15–16.00  $\mu\text{m}$ ) as well as the tritium concentration and hydrogen isotopic ratio ( $\delta\text{D}$ ). As the size of the dust influences its atmospheric lifetime, we divided the dust sizes into fine dust (FD) with diameters 0.52–1.00  $\mu\text{m}$ , coarse dust (CD) with diameters 1.00–8.00  $\mu\text{m}$ , and huge dust (HD) with diameters 8.00–16.00  $\mu\text{m}$ . Their characteristics and the reason why we defined these three ranges are discussed later. All the analyzing processes for the dust were identical to those in the previous study [*Fujii et al.*, 2003] except for the rinsing process for the samples using ultra pure water because the ice core was firm, and the estimated error in the dust analysis in this study was within 10%. We measured the tritium concentration for every 40 cm (total 124 samples) by using a liquid scintillation counter [*Kamiyama et al.*, 1997]. The analytical error was  $\pm 5\%$  in a 50 g and 7 TU sample, where the tritium unit

(TU) is given by  $1 \text{ TU} = 10^{-18} [^3\text{H}/\text{H}] = 0.1181 \text{ Bq/L}$ . The ratio  $\delta\text{D}$  was analyzed using the IsoPrime apparatus from Micromass [UK]. Measurements were made for every 10 cm for a total of 495 samples. The estimated measurement error was less than 0.1%.

We also carried out a field observation in May 2004 at the summit of Mount Wrangell. The snow samples were obtained approximately 3 times a day. The dust concentrations in these were analyzed with the same method as that for the ice core.

## 2.2. Trajectory analysis

A 10-day backward trajectory analysis was performed for the understanding of air mass transport routes to Mount Wrangell for the duration of the field observation at the summit in May 2004. A trajectory model was produced by *Yamazaki* [1986]. This trajectory model was constructed based on the Lagrangian tracking method. The horizontal and vertical wind data (3D wind data) from the Grid Point Values (GPV) data for May provided by the JMA were used for the calculations. The wind data were complemented by a linear interpolation into the horizontal wind data and a cubic spline interpolation into the vertical wind data. Air parcels were scattered in the space comprising a latitude line, longitude line, and vertical layer. The initial space was divided into 25 bins ( $5 \times 5$ ) horizontally and 5 layers vertically ( $5 \times 5 \times 5$ , total 125 bins). Abundant air parcel scatterings make reappearance of air mass pathways to Mount Wrangell better. Subsequently, one air parcel was scattered in each bin (total: 125 parcels). The calculation time step was 2 h. The initial space

centered on the summit of Mount Wrangell was set at 145.02°W–143.02°W in longitude, 60.59°N–62.59°N in latitude, and 700–500 hPa in altitude.

### 3. Results

#### 3.1. Ice-core dating

We use two important calibration layers for the ice-core dating. One is the drastic increase in the dust concentration in all the ranges at the depth from 26.824 to 26.873 m in water equivalent (hereafter denoted as m w.e.) due to Mt. Spurr Volcano's eruption in the fall of 1992. The other is the top of the ice core because we know that the drilling date was June 20, 2003. The ice core was drilled from a level of 0.85 m below the surface and the details will be discussed later.

The former was observed at the points labeled Y in Figure 2. The only visible sediment in the 50-m ice core was observed at this depth (Figure 3). The drastic increases in the dust concentrations were seen in the dust layer. The increases in FD, CD, and HD were larger by a factor of more than 100, 1000, and 10000 with regard to the mean values; the ash layer was excluded during the computation of the mean values in each range. These concentrations were abnormally higher than the background level in all ranges. In particular, the drastic HD increase suggests that a huge dust outbreak occurred very near the location. In 1992, the Crater Peak of Mount Spurr near Anchorage in Alaska erupted. The September 16-17 eruption ejected a large amount of volcanic ash and the trajectory analysis showed that the ash was transported to Mount Wrangell; the amount of dust deposition on the summit was presumed to be in the range from 50 to 100 g m<sup>-2</sup> in Figure 16 in the

work of *McGimsey et al.* [2002].

The preliminary results that were obtained using a petrographic microscope showed that the ash-layer samples were from the 1992 eruption of Crater Peak [*K. L. Wallace of USGS Anchorage, personal communication*]. A Comparison with the 1992 ash deposited in Anchorage showed petrographic and glass morphologic similarity to the ash samples in the ice core. The distances from Mount Spurr to Mount Wrangell and Anchorage are approximately 444 and 127 km, respectively.

Additionally, we calculated the mass of the ash deposition in the dust layer. The representative radius for each dust range, which was determined by the geometric mean between the minimum and maximum radius in the dust range, was used to calculate the single-particle volume. The single-particle mass at each range was then calculated with a typical mineral density of  $2600 \text{ kg m}^{-3}$  for each range. Subsequently, we estimated the amount of snow accumulation from the top of the dust layer to the bottom and the dust concentration in the dust layer. Finally, we obtained the total amount of ash deposition in all the dust ranges (0.52–16.00  $\mu\text{m}$ ) as  $77.34 \text{ g m}^{-2}$  by using the abovementioned data. This value was in the range from 50 to  $100 \text{ g m}^{-2}$  that was presumed by *McGimsey et al.* [2002]. In conclusion, the dust in the dust layer definitely corresponded to the Mount Spurr eruption. Taking into account all the abovementioned facts, we were convinced that the dust from the Mount Spurr eruption on 16–17 September 1992 was deposited onto the summit of Mount Wrangell.

If we take a look at the relationship of the ice-core data with the ash layer of Mount Spurr, we

can determine the seasons corresponding to certain depths. We used a running mean of five data points because the raw data greatly fluctuated over short distances, making it difficult to determine each peak depth. The  $\delta D$  minima sometimes had broad depths in Figure 2e; similar minimum values continued. Therefore, if more than two  $\delta D$  minima less than  $-240\text{‰}$  were found around the minima, we determined the minimum position in a certain year as the mean depth among the minimum peak depths.

Now, we know that the dust layer was deposited in September (fall). If we take a look around the ash layer, we find that just before the  $\delta D$  minimum peak depth the tritium concentration was decreasing from the maximum to the minimum. Therefore, the tritium minima are regarded as corresponding to the fall season, which occurred after 16-17 September (Mount Spurr eruption). The dust peak of Mount Spurr eruption also was seen between the maximum and minimum of  $\delta D$ , and the  $\delta D$  minima occurred after the tritium minima. Therefore, the  $\delta D$  maxima and minima are regarded as corresponding to summer and winter, respectively. This  $\delta D$  seasonal cycle was identical to that of  $\delta^{18}\text{O}$  at the nearest ice-core site, Eclipse Icefield ( $60.51^\circ\text{N}$ ,  $139.47^\circ\text{W}$ ; 3017 m a.s.l.) in the Saint Elias Range [Wake *et al.*, 2002]. Therefore, the  $\delta D$  data in our ice core also reflect past seasonal cycles and are similar to those of past ice-core studies [Holdsworth *et al.*, 1992; Thompson *et al.*, 2000; North Greenland Ice Core Project members, 2004].

The other dating point comprises the dust, tritium, and  $\delta D$  at the top layer of the ice core. The ice core was drilled in June 2003 from a depth of 0.85 m from the surface (0.207 m w.e.). If we

calculate the annual layer thickness by using  $\delta D$ , tritium, and FD and CD peaks, we obtain the annual mean snow accumulations from 2.43 to 2.58 m w.e. A snow accumulation of 0.207 m w.e. roughly corresponds to one month. Therefore, the ice-core data at the top roughly correspond to May. At the time, the concentration of FD and CD had just crossed their annual maxima, while that of tritium was located after the  $\delta D$  minimum and positioned near the maximum. We cannot determine whether the tritium concentration in the top layer was the maximum. The  $\delta D$  values in the top layer were almost the middle values between the minimum and the maximum in the annual cycles. The tritium concentrations and  $\delta D$  values before and after the Spurr eruption were consistent. All the tritium maxima occurred between the  $\delta D$  minima and maxima. Therefore, the tritium maxima are regarded as corresponding to springtime.

Moreover, we found that the CD maxima in Figure 2 appeared between the  $\delta D$  minima and the tritium maxima except for the year 2000 ( $X_1$  in Figure 2). Two possible origins of the CD are generally speculated. One is dust supply from a local source, while the other is dust transport from significant dust events in a remote place. Therefore, a seasonal pattern in the CD is not generally useful for intra-annual dating. However, it is useful to use the CD maxima for dating in this study because of clear seasonal positions between the  $\delta D$  minima and tritium maxima. Additionally, the correlation analysis between the FD and CD and field observations support the usefulness of dust seasonality as discussed later.

Among the three types of dust (FD, CD, and HD), the FD dominated the dust from distant

sources, presumably due to its long residence time in the atmosphere. When long-range transport from East Asia occurred, we observed that the FD increased in the field observation in May 2004 (Figure 4). This was verified by a 10-day backward trajectory model in which all 125 air parcels were scattered simultaneously [Yamazaki, 1986] (Figure 5). It indicates that the dust originated around the Gobi and Taklamakan deserts (Figure 5). In our data, we were generally able to identify a major CD or HD peak with a local dust-generating event, including volcanic eruptions; however, the CD levels also seasonally increased with the FD levels. For example, Figures 2a and 2b show that the FD and CD have similarly shaped broad peaks and minima, whereas the HD profile in Figure 2c has different characteristics.

These HD peaks are probably due to dust from volcanic plumes from the summit craters of Mount Wrangell when the wind was blowing from the north crater (Figure 4) because we observed a drastic increase in the HD characteristics at the summit in 2004 from 2-cm surface snow samples. Therefore, in the case of Mount Wrangell, the HD contributes the most to the dust variations in the ice core as its volcanic activities and the CD do not contribute significantly. After removing the peak from the Mount Spurr ash layers (symbol “Y” in Figure 2), the correlation coefficient between the FD and CD was calculated to be 0.62 (99.9% significance level; two-tailed t-test;  $n = 638$ ;  $t = 19.928$ ). It also indicates that the FD and CD outbreak events were mostly generated in the same place. Hence, the seasonal cycle of the CD is related with the FD variation.

We find that the depth positions for tritium and CD in 2000 in Figure 2 are inversely related,

which is an exceptional feature. The tritium and CD peaks for this year occurred only in early spring and late spring, respectively, because the tritium peaks were located before the CD peaks. With minor exceptions, we determined that the CD peaks mainly occur in early spring due to their clear seasonal positions. In conclusion, we will consider the CD maxima in Figure 2 as corresponding to early spring because almost all the CD peaks are located between the  $\delta D$  minima and tritium maxima. Moreover, we observe a 11-year maxima in the FD, CD, tritium, and  $\delta D$  and these maxima also fully explain the timing of the Y peaks in Figure 2 as being due to the dust event in 1992. Finally, we obtained the ice-core data, which spanned the years 1992–2002, that were divided into five seasons: early spring, late spring, summer, fall, and winter.

### 3.2. Dust and tritium fluxes in each season

To compare the annual trends in each season, we calculated the dust and tritium fluxes (Figure 6). The fluxes reflect all the dust and tritium increase events in each distinct season. The fluxes were calculated by multiplying the concentration of each element by the snow accumulation rate in each season. For the tritium fluxes, we considered the tritium half-life of 12.32 years [*Lucas and Unterweger, 2000*]. We used a representative month for each season in the calculation of tritium flux—April for early spring to late spring, June for late spring to summer, August for summer to fall, November for fall to winter, and February for winter to early spring. The HD was excluded from all further calculations because it is affected by the level of Mount Wrangell's volcanic activities.

Correlation analyses among the FD, CD, and tritium were done with the two-tailed t-test. The results between dust and tritium with a significance level greater than 90% are shown in Figure 6. Because tritium mainly exists as tritiated water vapor (HTO) in the atmosphere, snow deposition is more important than dry deposition. However, dust deposits occur either by dry deposition or with snow. For an ideal comparison between tritium and dust fluxes, we need to exclude data during abnormally large and small snow accumulations. We thus used the flux data in each divided season when the snow accumulations were within  $1\sigma$  of the mean values. Because we focused on the Asian dust contribution, we excluded the data from summer through winter of 1992 when the Mount Spurr eruption [McGimsey *et al.*, 2002] occurred. We excluded the data from the summer to the fall of 1998 too because large boreal forest fires occurred both in Siberia and Alaska in this year [Kasischke and Bruhwiler, 2002; M. Fukuda of ILTS, Hokkaido Univ., Japan, personal communication] and black carbon aerosol (soot) due to forest fires can be transported from central Alaska to southern Alaska glaciers [Kim *et al.*, 2005], probably corresponding to the drastic increase of FD from the summer to the fall of 1998 (Figure 2a). All the correlation matrixes among the FD, CD, and tritium fluxes and concentrations and snow accumulations in each season are also shown in Table 1.

By dividing the annual ice-core signals into signals corresponding to five distinct seasons, we obtained important data on the past atmospheric annual flux variations for each season (Figure 6). The amounts of dust and tritium in the atmosphere varied for each year and season. In springtime,

abnormally high FD and CD peaks were found after 2001 (Figures 2a, 2b, 6b, and 6e). It has been known that the outbreak frequency of Asian dust events is largest in March, April, and May. In particular, this has increased after the year 2000 [*Chun and Lim, 2004; JMA, 2004*]. Our results nicely support these two features and imply that Asian dust was definitely transported and deposited onto the summit of Mount Wrangell. Our backward trajectory analyses suggest that there are a lot of transport pathways from East Asia to Alaska and these vary with time. However, the background levels of dust concentration were particularly higher in springtime after 2001 (Figures 2a and 2b), implying that the Asian dust contribution to Mount Wrangell was significant. These flux increases in both the FD and CD were observed from the winter of 2000 to early spring of 2001 and from late spring to the summer of 2002 (Figures 2a, 2b, 6b, and 6e). This shows that severe dust events occurred in the springtime of 2001-2002 compared to those in the springtime of 1992–2000. The CD concentration in early spring of 2001 was the highest since 1992 except for the Mount Spurr eruption in 1992 (Figure 2b). Further, the FD concentration also increased together with the CD concentration (Figures 2a and 2b). This implies that the severest dust storm occurred in this year since 1992. Therefore, we can state that the atmosphere in early spring of 2001 was the most contaminated (both by the FD and CD) during the period 1992–2002.

The tritium concentration was high from early spring to summer and the highest in late spring in the raw data (Figure 2d). Tritium mainly exists as tritiated water vapor in the atmosphere, and prominent tritium peaks are detectable from spring to summer at the ground surface in the Northern

Hemisphere [Gat *et al.*, 2001]. Therefore, our results correspond to those of previous tritium studies. Most of the tritium that reaches the ground is produced in the stratosphere by cosmic rays and has a half-life of 12.32 years [Lucas and Unterweger, 2000]. Airborne tritium is also produced by nuclear tests. It has been used for determining the year 1962/1963 in ice-core researches [e.g., Fujii *et al.*, 1990] because of the massive tritium injections by the nuclear tests from 1961-1962 and the one- or two-year time lags of these effects. The tritium background level in the atmosphere has now returned to the level that existed before the nuclear tests [Gat *et al.*, 2001]. Therefore, the recent seasonal tritium variations in precipitation are mainly produced by cosmic rays in the stratosphere and intrusions from the stratosphere to the troposphere.

Tritium is exchanged between the troposphere and stratosphere by the stratosphere-troposphere exchange (STE). This process plays an important role in the material exchange (e.g., tritium and ozone) between the stratosphere and troposphere [Holton *et al.*, 1995; Monks, 2000; Gat *et al.*, 2001; Stohl *et al.*, 2003]. In this study, we use the term STE to refer to the one-way material intrusion from the stratosphere to the troposphere. The STE is actively generated through the tropopause folding by cutoff low, blocking high, or cyclonic activities [Holton *et al.*, 1995; Monks, 2000; Gat *et al.*, 2001; Stohl *et al.*, 2003]. The seasonal maximum of the STE is predominantly seen in springtime in the northern hemisphere [Holton *et al.*, 1995; Monks, 2000; Gat *et al.*, 2001; Stohl *et al.*, 2003]. The maximum concentration of stratospheric tracers such as tritium and ozone is also predominantly observed at the ground surface in springtime [Monks, 2000; Gat *et al.*, 2001].

Tritium has the highest concentrations north of 30° latitude [Gat *et al.*, 2001].

Two modifying processes delay the arrival of tritium at the ground surface by 26 days [Ehhalt, 1971]. One is the vertical transport process between high and low altitudes. The other is the re-evaporation of the winter and spring precipitation. The latter effect is dominant at altitudes below 3.05 km [Ehhalt, 1971]. Both effects contribute to the delay in the arrival of tritium at the ground surface. Due to the study location being at 4100 m, the delay caused by the vertical transport process may be the most important for tritium transport to Mount Wrangell. Therefore, tritium may be transported from the stratosphere to the summit of Mount Wrangell within one month.

We compared the tritium concentration at Mount Wrangell with the seasonal characteristics of tritium concentration in the precipitation at Anchorage, Alaska, by using the Global Network of Isotopes in Precipitation (GNIP) from the International Atomic Energy Agency (IAEA) and the World Meteorological Organization (WMO), Austria [IAEA/WMO, 2004] (Figure 7). Seasonal tritium peaks appeared from late spring to early summer (May–July) at Anchorage. Even if we consider a one-month delay at the ground surface as mentioned above, the tritium concentrations at the surface have maxima from early spring to summer (Figure 7). The tritium peaks in late spring in our ice-core results nicely correspond to those in the precipitation data; therefore, our ice-core results also reflect the seasonal cycle of tritium in the atmosphere. The tritium concentration and flux are the highest in late spring in Figures 2d and 6b, supporting the fact that tritium intrusions into the troposphere are the most active in late spring.

All the correlation coefficients with the two-tailed t-test among the fluxes and concentrations of FD, CD, and tritium and snow accumulations in each season were calculated within the limited period as mentioned earlier and are shown in Table 1. In the season from early spring to late spring (Table 1a), the FD and tritium fluxes were strongly correlated. The FD flux correlated with both the snow accumulation and the FD concentration, although the correlation between the FD concentration and flux was less than the 90% significance level. However, the correlation coefficient between the FD flux and concentration was similar in degree with the other high-significance correlations such as that between the dust and tritium fluxes or the dust flux and snow accumulation. It indicates that an annual relationship between the dust and tritium should exist between early and late spring. However, variations in the snow accumulation also strongly control this relationship. Hence, the annual relationship between the dust and tritium fluxes was observed due to the variations of dust and tritium concentrations and those of snow accumulation.

The tritium concentration and flux from early spring to late spring were highly correlated, indicating that the annual variation of tritium flux was due to variations in the concentration (Table 1a). The tritium flux was also correlated with snow accumulation, indicating that the snow effectively decreased the tritium background level in the atmosphere in this season. This is reasonable because tritium existed as tritiated water vapor in the atmosphere as mentioned above and therefore may have an increased affinity to snow or wet depositions rather than dry depositions.

In the season from late spring to summer, the fluxes of FD and tritium had the highest

correlation (Table 1b). These also had high correlations with the concentrations of FD and tritium, CD flux, and the snow accumulation, indicating that the strong annual variations of the FD and tritium fluxes were due to both the variations in the concentration and the snow accumulation. However, the CD flux was not highly correlated with the snow accumulation. Therefore, the annual variations of both the FD and tritium fluxes were associated with snow deposition and that of the CD was associated with the dry deposition in this season (late spring to summer). It indicates that FD from a remote place may contribute to the annual relationship between dust and tritium. This is an interesting feature. In conclusion, the FD had the strongest annual relationship with tritium in this season.

In the season from summer to fall, the FD and CD were correlated only with snow accumulation (Table 1c) because the increases in dust and tritium were small and this season is the summer rainy season in Alaska [Polissar *et al.*, 1998]. Hence, the mean atmospheric dust levels were almost constant in this season from 1993 to 2002 and the amount of snowfall controlled the amount of dust deposition.

In the season from fall to winter, snow accumulation did not contribute to the flux variations significantly and variations in the concentrations of FD, CD, and tritium contributed the most to the fluxes (Table 1d). Therefore, the variations in the concentrations strongly controlled the annual flux variations.

In the season from winter to early spring, the FD and CD fluxes were correlated with their

concentrations (Table 1e). However the correlations for tritium were weak, indicating that the annual variations of the dust fluxes depended on variations in their concentrations and that of tritium depended on the snow accumulation in this season.

### 3.3. Comparison of dust deposition amount in Alaska with those in other areas

We calculated the annual mean and seasonal mean of the dust particle number density, dust mass, and fluxes with the same method that was used in sections 3.1 and 3.2, as shown in Table 2. The abbreviations for ES, LS, SU, FA, and WI in Table 2 denote early spring, late spring, summer, fall, and winter, respectively. The dust size range 8–16  $\mu\text{m}$  was excluded because Mount Wrangell's volcanic activities contributed the most in this range as mentioned above. Table 2 was originally produced by *Zdanowicz et al.* [1998] and we added our results to it. The Mount Spurr eruption strongly contributed to the mass deposition. However, if we exclude it, the values were less than those observed in China [*Wake et al.*, 1994]. The annual mean mass in this study was the same as that for the Alaskan range near Mount Wrangell [*Hinkley*, 1994]. The range of the dust flux for Mount Wrangell was the same as those of the Canadian Basin and Saint Elias Range (USA) [*Windom*, 1969; *Mullen et al.*, 1972; *Darby et al.*, 1974]. Greenland and Canadian Arctic were cleaner than our site [*Murozumi et al.*, 1969; *Kumai*, 1977; *Hammer*, 1977; *Fisher and Koerner*, 1981; *Koerner and Fisher*, 1982; *Hammer et al.*, 1985; *Steffensen*, 1988; *Steffensen*, 1997; *Zdanowicz et al.*, 1998]. However, the seasonal means of the mass from late spring to fall for Mount

Wrangell were similar to the annual means in Canadian Arctic and larger by a factor of 2–3 as compared to Greenland. The contamination in the atmosphere around the summit of Mount Wrangell was higher in spring than in the season from summer to fall by a factor of 4. With regard to the history of dust studies in the Northern Hemisphere, the annual mean value in this study corresponded to those of the Younger Dryas event and the post-Last Glacial Maximum in Greenland, and the seasonal mean value in springtime (WI-ES and ES-LS) in the present ice core agreed with that of the Eemian event 2 [Steffensen, 1997].

## 4. Discussion

### 4.1. Dust characteristics for each defined range and their origins

Dust concentration in the FD and the CD ranges showed clear seasonal variations (Figure 2), and these two ranges were closely correlated with each other as mentioned in section 3.1. In the Mount Wrangell ice core, we determined that the dust maxima in Figure 2 corresponded to early spring. Previous studies have mentioned that soil aerosols in Alaska increase the most in April [Malm *et al.*, 1994; Malm *et al.*, 2004]. The Si variation also has spring maxima in Alaska [Polissar *et al.*, 1998]. These previous results were obtained from the Interagency Monitoring of Protected Visual Environments (IMPROVE) network (<http://vista.cira.colostate.edu/IMPROVE/>); this network was established by an interagency consortium of federal land management agencies and the Environmental Protection Agency in the spring of 1985 to assess visibility and aerosol

monitoring for the purpose of tracking spatial and temporal trends of visibility and visibility-impairing particles in rural areas. A sample of the IMPROVE data in Alaska at Denali National Park (63.72°N, 148.97°W, 658 m a.s.l.; highest site in Alaska) is shown in Figure 8, which is calcium data for particles less than 2.5  $\mu\text{m}$ . The Ca data mainly have distinctive spring maxima; however, they sometimes have additional peaks corresponding to another season. Our result for the early spring maxima in the FD and CD corresponds to the seasonal variations in Figure 8. Therefore, our results for the dust at the summit of the mountain may also represent the typical seasonal variation of the atmospheric soil dust in Alaska.

We discuss the origins of dust in springtime in the following. First, we consider two typical origins. One is from a local area in Alaska. The other is due to transport from a remote area in the world. *Polissar et al.* [1998] mentioned that Alaskan time periods had been divided according to different synoptic conditions in the Arctic as follows. Spring from March to June is associated with a period of intensive long-range transport and effective photochemical transformation of aerosols in the Arctic troposphere during polar sunrise. Summer from July to September is related to a period of low long-range transport and more effective scavenging processes by precipitation and clouds. Winter from October to February is represented by a transitional synoptic situation. Therefore, it is known in Alaska that long-range transport is dominant in springtime and not dominant in summer because of the summer rainy season. In fact, in our results, the FD concentration increases the most in springtime due to long-range transport, as shown in Figure 2, and both the FD and CD flux are

correlated with the snow accumulation only from summer to fall in Table 1, indicating that wet deposition is the most dominant in this season. Our drilling site is located at a high altitude and synoptic atmospheric circulations may influence the summit directly. The long-range transport of FD from East Asia was actually observed at the summit in the field observation (Figures 4 and 5). The case of long-range transport showed one example of a typical springtime pattern for material transport from East Asia. It is presumed that the seasonal FD and CD cycles are due to dust outbreak events in remote places. Of course, dust from local areas near Mount Wrangell may contribute to the variation of the CD in the ice core to some extent. However, we assumed that the clear seasonal cycles of dust mainly depend on contributions from remote areas because the FD generally has a long residence time and the FD and CD were highly correlated with regard to their seasonal cycle.

For long-range transport of the CD, a stronger wind velocity as compared to the FD is required to cover the required distance in the atmosphere. Additionally, the CD needs to reach a higher altitude because long-range transport by the westerly jet occurs in the free troposphere. It was pointed out by *Sun et al.* [2001] that cold fronts with a strong wind velocity were important in springtime for the long-range transport of dust and the dust of the Taklamakan Desert contributed more to the long-range transport as compared to that of the Gobi Desert. The maxima of the FD and CD were observed in early spring with a high positive correlation in our dating (Figures 2a and 2b). In this season, the main sources of dust from East Eurasia to the North Pacific are the Gobi and

Taklamakan deserts and arid regions in East Asia. These deserts are known to have frequent dust storms in springtime [*Sun et al.*, 2001]. A strong vertical convection and high wind speeds at the ground surface are needed to lift dust to the altitude of the strong westerly jet.

Long-range transport of Asian dust over the Pacific Ocean has been observed [*Rahn et al.*, 1977; *McKendry et al.*, 2001; *VanCuren and Cahill*, 2002; *Cahill*, 2003; *Darmenova et al.*, 2005]. In the springtime of 2001, the CD dust concentrations and fluxes increased the most in the ice core (Figures 2b and 6e); The FD also increased together (Figure 2a). In fact, severe dust storms occurred in East Asian deserts and large amounts of dust were transported to the North Pacific and Alaska [*Yu et al.*, 2003; *Zhang et al.*, 2003; *Darmenova et al.*, 2005]. The Sea-viewing Wide Field-of-view Sensor (SeaWiFS) images also showed abnormally large and long-lasting dust clouds in April 2001 (NASA science news, 17 May 2001 at <http://science.nasa.gov/headlines/>). In the article, Herman, the principal investigator of NASA's Total Ozone Mapping Spectrometer (TOMS) experiment, mentioned that in terms of the area covered, this was the largest dust storm observed in the Northern Hemisphere since 1979. The largest Asian dust storm broke out on April 6-7, 2001 and its large dust cloud reached Alaska on April 13, 2001 (see the web site of Visible Earth: [http://visibleearth.nasa.gov/view\\_rec.php?id=14051](http://visibleearth.nasa.gov/view_rec.php?id=14051)). Although our ice core covers the years from 1992 to 2002, the CD maximum in the spring of 2001 in Figure 2b is undoubtedly the largest after 1992, except for the eruption of Mount Spurr and probably corresponds to the dust storm from East Asia. In the case of northern Chinese deserts during this spring, the peak mass loading occurred for

the range of 4 to 8  $\mu\text{m}$  in most dust-storm cases and these dust storms were commonly associated with dry and windy conditions [Zhang *et al.*, 2003]. The dominant dust range corresponds to our CD range. Of course, generally, CD has a lower residence time in the atmosphere as compared to FD. However, the contribution of the westerly jet to the long-range transport of dust to Mount Wrangell is large as mentioned above. Therefore, we cannot exclude the contribution of the Asian dust; it is also not possible to explain the clear seasonal variations in the CD that are associated with those of the FD at altitudes greater than 4000 m in the free troposphere without the Asian dust contribution. Therefore, we propose that a site at a high altitude, like the summit of Mount Wrangell, is largely affected by the Asian dust in the springtime every year; this is also true for other places in Alaska and regions around the northeast Pacific Basin and Canada [Rahn *et al.*, 1977; McKendry *et al.*, 2001; VanCuren and Cahill, 2002; Cahill, 2003].

In the North Pacific region, ice-core results are still sparse. However, dust loading is large in this area and various transport models have calculated the dust distribution and transport pattern [e.g., Takemura *et al.*, 2002; Uno *et al.*, 2003; Tanaka *et al.*, 2005]; however, information on the actual dust deposition is desirable. In particular, this importance is larger with regard to the past for which there is no meteorological data. Therefore, our intraseasonal dust data in the ice core may contribute to these demands, enabling an assessment of the past seasonal climate phenomena.

#### 4.2. Seasonal variation of tritium in the troposphere

26

Yasunari *et al.*, *J. Geophys. Res.*, published 19 May 2007.

An edited version of this paper was published by AGU.

Copyright (2007) American Geophysical Union.

We obtained the maximum tritium concentration in late spring, except for the year 2000 (early spring), for the period from 1992 to 2002 (Figure 2d). The observed precipitation data near the ground surface depicted in Figure 7 also showed similar seasonal variations. Therefore, the seasonal variation of tritium with the maximum in late spring may be a typical phenomenon in this region. The origin of tritium in recent years is mainly from the stratosphere where it is produced by cosmic rays; tritium that resulted from the effect of thermonuclear tests has disappeared [Gat *et al.*, 2001]. Although the half-life of tritium is short (12.32 years [Lucas and Unterweger, 2000]), we can detect the seasonal cycle till the year 1963, which is one year after the year of a thermonuclear test. This anthropogenic effect may help to reconstruct the seasonal variation as a visible variation in the concentration and compensate the half-life decay. After around 1980, tritium concentration levels have been returning to pre-1963 values [Gat *et al.*, 2001]. Hence, the effects of nuclear tests have almost disappeared since 1980 and the seasonal variation of tritium after 1980 may mainly be due to their production by cosmic rays in the stratosphere and their intrusion into the troposphere in springtime. In conclusion, in the ice-core study at Mount Wrangell, tritium is very useful to determine the late spring period if a time resolution is sufficient for about one month.

#### 4.3. Comparison among dust and tritium fluxes

We examined the strength of the annual relationship between tritium and the dust fluxes. The highest positive correlation (98% significance level; two-tailed t-test) occurred in late spring

through summer in the case of tritium and FD fluxes (Figure 6b). This suggests that the long-range transport of FD and the amount of STE may be related on an annual basis and strongest in late spring because the STE and strong frontal storms with Asian dust outbreaks are the most active in springtime and the weakest in summer [Holton *et al.*, 1995; Monks, 2000; Gat *et al.*, 2001; Sun *et al.*, 2001; Stohl *et al.*, 2003; Chun and Lim, 2004; JMA, 2004]. The drastic increases in the FD and CD fluxes after 2000 (Figures 6b and 6e) coincide with the recent increase in Asian dust outbreaks [Chun and Lim, 2004; JMA, 2004]. As discussed in section 4.1., the contribution of Asian dust in springtime may be large in this region. For such a long-range transport of dust, the Asian dust must be lifted up to the altitude of the strong westerly jet by severe weather at the ground surface and a strong vertical convection. The severe weather such as strong cyclonic activities also contributes to the STE [Browning and Reynolds, 1994]. Further, the air from the stratosphere into the troposphere may tend to increase in strength, and an increase in stratospheric tracers such as tritium and ozone might be observed near the ground surface; an example is the case of ozone increase in East Asia with the Asian dust storm [Kim *et al.*, 2002]. The annual relationship between the STE and strong frontal storms with Asian dust outbreaks is weak, except for the seasons from early spring to late spring in Figures 6a and 6b; this indicates that the contribution of strong frontal storms with Asian dust outbreak to the STE is the largest in late spring. Hence, we propose that the annual relationship between the STE and strong cyclonic activities with Asian dust outbreaks may be the strongest in late spring (Figure 9).

Although there have been many studies on the Asian dust and the STE independently, there have been no studies on the annual relationship between the strong frontal storms with Asian dust outbreaks and STE because it has been difficult to obtain observations at a single location for several years. Because ice cores continuously preserve the past atmospheric information, it is possible to detect the relationship for several years. Unfortunately, our results are still not sufficient to fully discuss the annual relationship between the STE and strong cyclonic activities with Asian dust outbreaks because the STE mostly occurs on a few days; however, our timely high-resolution data for the dust and tritium roughly correspond to one week and one month, respectively. Of course, we also cannot know the locations where the STE occurred from only the ice-core results. However, the flux data reflect all the seasonal atmospheric dust and tritium events and our results suggest that Asian dust effect to Mount Wrangell in springtime is evident. Therefore, our speculation is probable and we suggest that this study is the first step to assess the annual relationship between the STE and strong frontal storms with Asian dust outbreaks; henceforth, we should monitor this relationship over a longer time because it leads to various climate changes due to intrusions of the stratospheric tracer into the troposphere and also causes changes in the radiative balance due to an increase in the dust in the troposphere. More studies involving field observations and model studies are necessary and in the near future they will elucidate the annual relationship between the STE and strong cyclonic activities with Asian dust outbreaks and assess their influence on climate change.



## 5. Conclusions

By analyzing an ice core from the summit of Mount Wrangell with an intra-annual dating resolution, we obtained data for clear seasonal variations in  $\delta D$ , tritium, and dust from 1992 to 2002. We succeeded in dating the intra-annual layers and divided each year into five distinct seasons to show the clear annual variations of tritium and dust for each season. The parameter  $\delta D$  has summer maxima and winter minima. The FD and CD concentrations were strongly correlated and had early spring maxima, and Asian dust storms in springtime may strongly contribute to the seasonal variations of the dust. The annual mean dust deposition flux (Table 2) at the summit of Mount Wrangell, which is in the free troposphere, was larger than that for the Canadian Arctic and Greenland; less than that for China, Nepal, France, and USA mainland; and similar to that for the Arctic Ocean. The tritium in the ice core had a late spring maximum and fall minimum and its fluxes had the highest annual correlation with the FD fluxes in the late spring season. Subsequently, the strongest annual link between Asian dust storms and the STE may occur in late spring. However, the time resolution of our ice-core data and the analysis for transport pathways in springtime are still not sufficient for a full discussion, and more studies are necessary in the future. Our result is the first step in the study on the annual relationship between Asian dust storms and the STE. The number of days on which Asian dust storms have been observed in East Asia has been increasing recently [*Chun and Lim*, 2004; *JMA*, 2004]; this may not only increase the dust in the atmosphere but also the amount of STE depending on our result that FD and tritium fluxes were annually

correlated in late spring the most (Figure 9). This can lead to an increase in tritium and ozone in the troposphere. More studies in the future on both the STE and Asian dust will explain this.

In the North Pacific region, a seasonal variation in the climate is evident. Therefore, seasonal datasets of ice cores are necessary to reconstruct the past climate here. However, such datasets in the North Pacific region are still sparse. We fortunately succeeded in intra-annual dating with 5 seasons in this region. If we analyze longer ice cores drilled at the summit of Mount Wrangell and covering several hundred years, we can present detailed discussions on intra-annual climate changes in the past for which there is no meteorological data. The Mount Wrangell ice core will also contribute considerably to paleoclimate studies and model researches on dust circulation around the North Pacific involving probable features on intra-annual time scales. Our preliminary results in this study have covered only the recent 11 years, but the results will contribute to further studies.

## Acknowledgments

This research was supported by a Grant-in-Aid for Creative Scientific Research (No. 14GS0202) and Basic Research B (No.16403005) from the Japanese Ministry of Education, Culture, Sports, Science and Technology. Tephra samples in the ice core were analyzed by Kristi Wallace of USGS Anchorage. Forest fire data in Siberia and Alaska was provided from Masami Fukuda of ILTS, Hokkaido University, Japan. Tritium data at Anchorage (Alaska) was obtained from the United States Geological Survey, Reston, VA, USA. The IMPROVE data at Denali National Park were monitored by the U.S. National Park Service. The GPV 3D wind data were provided from the server blade of the Course in Atmosphere-Ocean & Climate Dynamics of the Graduate School of Environmental Science, Hokkaido University, Japan. Dust and tritium were analyzed at the National Institute of Polar Research (NIPR), Japan. Dust and tritium analyses were supported by Tomoko Naka and Maki Nakada at NIPR. We appreciate all the institutions and the personnel as mentioned above for their support.

## References

- Benson, C. S., and R. J. Motyka (1978), Glacier-volcano interaction on Mt. Wrangell, Alaska, *Geophysical Institute Annual Report*, 1–25.
- Bjerknes, J. (1969), Atmospheric teleconnections from the Equatorial Pacific, *Mon. Wea. Rev.*, *97*, 163–172.
- Browning, K. A., and R. Reynolds (1994), Diagnostic study of a narrow cold-frontal rainband and severe winds associated with a stratospheric intrusion, *Q. J. R. Meteorol. Soc.*, *120*, 235–257.
- Cahill, C. F. (2003), Asian aerosol transport to Alaska during ACE-Asia, *J. Geophys. Res.*, *108*(D23), 8664, doi:10.1029/2002JD003271.
- Chun, Y., and J.-Y. Lim (2004), The recent characteristics of Asian dust and haze events in Seoul, Korea, *Meteorol. Atmos. Phys.*, *87*, 143–152.
- Darby, D. A., L. H. Burckle, and D. L. Clark (1974), Airborne dust on the Arctic ice pack, its composition and fallout rate, *Earth Planet. Sci. Lett.*, *24*, 166–172.
- Darmenova, K., I. N. Sokolik, and A. Darmenov (2005), Characterization of east Asian dust outbreaks in the spring of 2001 using ground-based and satellite data, *J. Geophys. Res.*, *110*, D02204, doi:10.1029/2004JD004842.
- De Angelis, M., and A. Gaudichet (1991), Saharan dust deposition over Mont Blanc (French Alps) during the last 30 years, *Tellus*, *43B*, 61–75.

Ehhalt, D. H. (1971), Vertical profiles and transport of HTO in the troposphere, *J. Geophys. Res.*, *76*, 7351–7367.

Fisher, D. A., and R. M. Koerner (1981), Some aspects of climatic change in the high Arctic during the Holocene as deduced from ice cores, in *Quaternary Paleoclimate*, edited by W. C. Mahaney, pp. 249–271, University of East Anglia Press, Norwich.

Fujii, Y., et al. (1990), 6000-Year climate records in an ice core from the Høghetta Ice Dome in northern Spitsbergen, *Ann. Glaciol.*, *14*, 85–89.

Fujii, Y., M. Kohno, S. Matoba, H. Motoyama, and O. Watanabe (2003), A 320 k-year record of microparticles in the Dome Fuji, Antarctica ice core measured by laser-light scattering, *Mem. Natl Inst. Polar Res., Spec. Issue*, *57*, 46–62.

Gat, J. R., W. G. Mook, and H. A. J. Meijer (2001), Tritium in the atmosphere, in *Atmospheric Water: Environmental Isotopes in the Hydrological Cycle Principles and Applications*, vol. II, edited by W. G. Mook, pp. 63–74, UNESCO/IAEA Series, Paris. (Available at: <http://www.iaea.org/programmes/ripc/ih/volumes/volumes.htm>.)

Hammer, C. U. (1977), Dust studies on Greenland ice cores, in *Isotopes and Impurities in Snow and Ice*, pp. 365–370, International Association of Hydrological Sciences, Grenoble.

Hammer, C. U., H. B. Clausen, W. Dansgaard, A. Neftel, P. Kristinsdottir, and E. Johnson (1985), Continuous impurity analysis along the Dye 3 deep core, in *Greenland Ice Core: Geophysics, Geochemistry and the Environment*, *Geophys. Monogr.*, edited by C. C.

Langway Jr., H. Oeschger and W. Dansgaard, pp. 90–94, AGU, Washington, D. C.

Hinkley, T. D. (1994), Composition and sources of atmospheric dust in snow at 3200 meters in the St. Elias Range, southeastern Alaska, USA, *Geochim. Cosmochim. Acta*, *58*, 3245–3254.

Holdsworth, G., H. R. Krouse, and M. Nosal (1992), Ice core climate signals from Mount Logan, Yukon, A.D. 1700–1987, in *Climate Since A.D. 1500*, edited by R. S. Bradley and P. D. Jones, pp. 483–504, Routledge, London.

Holton, J. R., P. H. Haynes, M. E. McIntyre, A. R. Douglass, R. B. Rood, and L. Pfister (1995), Stratospheric troposphere exchange, *Rev. Geophys.*, *33*, 403–439.

IAEA/WMO (2004), Isotope Hydrology Information System, *The ISOHIS Database*, International Atomic Energy Agency, Vienna, Austria. (Accessible at: <http://isohis.iaea.org>.)

Iwasaka, Y., H. Minoura, and K. Nagaya (1983), The transport and spacial scale of Asian dust-storm clouds: a case study of the dust-storm event of April 1979, *Tellus*, *35B*, 189–196.

Japan Meteorological Agency (2004), Basic knowledge about Asian dust (Kosa). (Available at the website in Japanese: <http://www.data.kishou.go.jp/obs-env/hp/4-4kosa.html>.)

Kamiyama, K., W. Shimada, K. Kitaoka, K. Izumi, and S. Ezumi (1997), Determination of HTO content in polar ice/snow samples by low background liquid scintillation technique, *Nankyoku Shiryo (Antarctic Record)*, *41*, 631–642.

Kanamori, S. (2004), Seasonal variations in density profiles at cold mountain glaciers, M. S. thesis,

68 pp., Hokkaido University, Sapporo.

Kasischke, E. S., and L. P. Bruhwiler (2002), Emission of carbon dioxide, carbon monoxide, and methane from boreal forest fires in 1998, *J. Geophys. Res.*, *108*(D1), 8146, doi:10.1029/2001JD000461.

Kim, Y., H. Hatsushika, R. R. Muskett, and K. Yamazaki (2005), Possible effect of boreal wildfire soot on Arctic sea ice and Alaska glaciers, *Atmos. Environ.*, *39*, 3,513-3,520.

Kim, Y. K., H. W. Lee, J. K. Park, and Y. S. Moon (2002), The stratosphere-troposphere exchange of ozone and aerosols over Korea, *Atmos. Environ.*, *36*, 449–463.

Koerner, R. M., and D. A. Fisher (1982), Acid snow in the Canadian High Arctic, *Nature*, *295*, 137–140.

Kumai, M. (1977), Electron microscope analysis of aerosols in snow and deep ice cores from Greenland, in *Isotopes and Impurities in Snow and Ice*, pp. 341–350, International Association of Hydrological Sciences, Grenoble.

Lucas, L. L., and M. P. Unterweger (2000), Comprehensive review and critical evaluation of the half-life of tritium, *J. Res. Natl. Stand. Technol.*, *105*(4), 541–549.

Malm, W. C., B. A. Schichtel, M. L. Pitchford, L. L. Ashbaugh, and R. A. Eldred (2004), Spatial and monthly trends in speciated fine particle concentration in the United States, *J. Geophys. Res.*, *109*, D03306, doi:10.1029/2003JD003739.

Malm, W. C., J. F. Sisler, D. Huffman, R. A. Eldred, and T. A. Cahill (1994), Spatial and seasonal

trends in particle concentration and optical extinction in the United States, *J. Geophys. Res.*, **99**(D1), 1347–1370.

Mantua, N. J., S. R. Hare, Y. Zhang, J. M. Wallace, and R. C. Francis (1997), A Pacific interdecadal climate oscillation with impacts on salmon production, *Bull. Amer. Meteorol. Soc.*, **78**(6), 1069–1079.

McGimsey, R. G., C. A. Neal, and C. M. Riley (2002), Areal distribution, thickness, mass, volume, and grain size of tephra-fall deposits from the 1992 eruptions of Crater Peak Vent, Mt. Spurr Volcano, Alaska, *Open File Rep. 01-370*, 38 pp., U.S. Geol. Surv, Denver, CO, USA. (Available at : <http://geopubs.wr.usgs.gov/open-file/of01-370/>.)

McKendry, I. G., J. P. Hacker, R. Stull, S. Sakiyama, D. Mignacca, and K. Reid (2001), Long-range transport of Asian dust to the Lower Fraser Valley, British Columbia, Canada, *J. Geophys. Res.*, **106**(D16), 18,361–18,370.

Monks, P. S. (2000), A review of the observations and origins of the spring ozone maximum, *Atmos. Environ.*, **34**, 3545–3561.

Mullen, R. E., D. A. Darby, and D. L. Clark (1972), Significance of atmospheric dust and ice rafting from Arctic Ocean sediment, *Geol. Soc. Amer. Bull.*, **83**, 205–212.

Murozumi, M., T. J. Chow, and C. Patterson (1969), Chemical concentrations of pollutant lead aerosols, terrestrial dusts and sea salts in Greenland and Antarctic snow strata, *Geochim. Cosmochim. Acta*, **33**, 1247–1294.

- North Greenland Ice Core Project members (2004), High-resolution record of Northern Hemisphere climate extending into the last interglacial period, *Nature*, *431*, 147–151.
- Polissar, A. V., P. K. Hopke, W. C. Malm, and J. F. Sisler (1998), Atmospheric aerosol over Alaska, 1. Spatial and seasonal variability, *J. Geophys. Res.*, *103*(D15), 19,035–19,044.
- Rahn, K. A., R. D. Borys, and G. E. Shaw (1977), Asian source of Arctic haze bands, *Nature*, *268*, 713–715.
- Rahn, K. A., R. D. Borys, G. E. Shaw, L. Schütz, and R. Jaenicke (1979), Long-range impact of desert aerosol on atmospheric chemistry: two examples, in *Saharan Dust: Mobilization, Transport, and Deposition*, edited by C. Morales, pp. 243–266, J. Wiley, New York.
- Shiraiwa, T., Y.D. Muravyev, T. Kameda, F. Nishio, Y. Toyama, A. Takahashi, A.A. Ovsyannikov, A.N. Salamatin and K. Yamagata (2001), Characteristics of a crater glacier at Ushkovsky volcano, Kamchatka, Russia, as revealed by the physical properties of ice cores and borehole thermometry. *J. Glaciol.*, *47*, 423-432.
- Shiraiwa, T., K. Goto-Azuma, S. Matoba, T. Yamasaki, T. Segawa, S. Kanamori, K. Matsuoka, Y. Fujii (2003), Ice core drilling at King Col, Mount Logan 2002, *Bull. Glaciol. Res.*, *20*, 57–63.
- Shiraiwa, T., S. Kanamori, C. S. Benson, D. Solie, and Y. D. Muravyev (2004), Shallow ice-core drilling at Mount Wrangell, Alaska, *Bull. Glaciol. Res.*, *21*, 71–77.

- Steffensen, J. P. (1988), Analysis of the seasonal variation in dust,  $\text{Cl}^-$ ,  $\text{NO}_3^-$ , and  $\text{SO}_4^{2-}$  in two central Greenland firn cores, *Ann. Glaciol.*, *10*, 171–177.
- Steffensen, J. P. (1997), The size distribution of microparticles from selected segments of the Greenland Ice Core Project ice core representing different climatic periods, *J. Geophys. Res.*, *102(C2)*, 26,755–26,763.
- Stohl, A., et al. (2003), Stratosphere-troposphere exchange: A review, and what we have learned from STACCATO, *J. Geophys. Res.*, *108(D12)*, doi:10.1029/2002JD002490.
- Sun, J., M. Zhang, and T. Liu (2001), Spatial and temporal characteristics of dust storms in China and its surrounding regions, *J. Geophys. Res.*, *106(D10)*, 10,325–10,333.
- Takemura, T., I. Uno, T. Nakajima, A. Higurashi, and I. Sano (2002), Modeling study of long-range transport of Asian dust and anthropogenic aerosols from East Asia, *Geophys. Res. Lett.*, *29(24)*, 2158, doi:10.1029/2002GL016251.
- Tanaka, T. Y., and M. Chiba (2005), Global simulation of dust aerosol with a chemical transport model, MASINGAR, *J. Meteorol. Soc. Jpn.*, *83A*, 255–278.
- Thompson, D. W., and J. M. Wallace (1998), The Arctic Oscillation signature in the wintertime geopotential height and temperature fields, *Geophys. Res. Lett.*, *25(9)*, 1297–1300.
- Thompson, L. G., T. Yao, E. Mosley-Thompson, M. E. Davis, K. A. Henderson, and P. -N. Lin (2000), A high-resolution millennial record of the South Asian monsoon from Himalayan ice cores, *Science*, *289*, 1916–1919.

- Uno, I. et al. (2003), Regional chemical weather forecasting system CFORS: Model descriptions and analysis of surface observations at Japanese island stations during the ACE-Asia experiment, *J. Geophys. Res.*, *108*(D23), 8668, doi:10.1029/2002JD002845.
- VanCuren, R. A., and T. A. Cahill (2002), Asian aerosols in North America: frequency and concentration of fine dust, *J. Geophys. Res.*, *107*(D24), 4804, doi:10.1029/2002JD002204.
- Wagenbach, D., and K. Geiss (1989), The mineral record in a high altitude alpine glacier (Colle Gnifetti, Swiss Alps), in *Paleoclimatology and Paleometeorology: Modern and Past Patterns of Global Atmospheric Transport*, edited by M. Leinen and M. Sarnthein, pp. 543–564, Kluwer Academic Publishers, Dordrecht.
- Wake, C. P., P. A. Mayewski, Z. Li, J. Han, and D. Qin (1994), Modern eolian dust deposition in Central Asia, *Tellus*, *46B*, 220–233.
- Wake, C. P., K. Yalcin, and N. S. Gundestrup (2002), The climate signal recorded in the oxygen-isotope, accumulation and major-ion time series from the Eclipse ice core, Yukon Territory, Canada, *Ann. Glaciol.*, *35*, 416–422.
- Windom, H. L. (1969), Atmospheric dust records in permanent snowfields: implications to marine sedimentation, *Geol. Soc. Amer. Bull.*, *80*, 761–782.
- Yamazaki, K. (1986), Preliminary calculation of trajectory analysis in the lower stratosphere of the Southern Hemisphere, *Geophys. Res. Lett.*, *13*, 1312–1315.
- Yu, H., R. E. Dickinson, M. Chin, Y. J. Kaufman, B. N. Holben, I. V. Geogdzhayev, and M. I.

Mishchenko (2003), Annual cycle of global distributions of aerosol optical depth from integration of MODIS retrievals and GOCART model simulations, *J. Geophys. Res.*, *108*(D3), 4128, doi:10.1029/2002JD002717.

Zdanowicz, C. M., G. A. Zielinski, and C. P. Wake (1998), Characteristics of modern atmospheric dust deposition in snow on the Penny Ice Cap, Baffin Island, Arctic Canada, *Tellus*, *50B*, 506–520.

Zhang, X. Y., S. L. Gong, R. Arimoto, Z. X. Shen, F. M. Mei, D. Wang, and Y. Cheng (2003), Characterization and Temporal Variation of Asian Dust Aerosol from a Site in the Northern Chinese Deserts, *J. Atmos. Chem.*, *44*, 241–257.

## Figure Captions

**Figure 1.** Schematic depiction of the summit of Mount Wrangell (elevation: 4100 m). The large picture is an aerial photograph at the summit taken by AeroMap, Anchorage, US. The summit caldera shapes a  $4 \times 6$  km oblong crown and has 1 km deep [Shiraiwa *et al.*, 2004].

**Figure 2.** Dust, tritium, and  $\delta D$  variations in the Mount Wrangell ice core. Concentrations in the **(a)** fine dust (FD) ( $0.52\text{--}1.00 \mu\text{m}$ ); **(b)** coarse dust (CD) ( $1.00\text{--}8.00 \mu\text{m}$ ); and **(c)** huge dust (HD) ( $8.00\text{--}16.00 \mu\text{m}$ ). **(d)** Tritium concentration. **(e)** Ratio of stable hydrogen isotope ( $\delta D$ ). Depth was converted to water equivalent depth by using the density profiles [Kanamori, 2004]. Circles, triangles, squares, reverse-triangles, and stars denote the approximate positions of early spring, late spring, summer, fall, and winter, respectively, and each symbol is placed next to the curve that was used in their determination. The symbols  $X_1$  (circle) and  $X_2$  (triangle) mark late spring and early spring in 2000, respectively. The vertical solid lines of orange, yellowish green, yellow, violet, and sky-blue also denote early spring, late spring, summer, fall, and winter, respectively. The intervals between same colored vertical solid lines delineate annual increments. Symbol Y in **(a)**, **(b)**, and **(c)** corresponds to the clear dust layer from 26.824 to 26.873 m in water equivalent. The error bars in **(e)** denote broad minima which were used to determine the center depths in winter as mentioned in section 3.1. All the bold blue lines denote running means of 5 data points. The horizontal lines

denote  $-240\text{‰}$  level of  $\delta\text{D}$ .

**Figure 3.** The picture of the ash layer corresponds to Mount Spurr eruption on 16-17 September in 1992 at a core depth of 26.824 to 26.873 m in water equivalent. The clear ash layer was found only at this depth in the ice core.

**Figure 4.** Dust content in the uppermost 2 cm of surface snow at the summit. Variations of FD, CD, and HD were measured about 3 times per day.

**Figure 5.** Air mass trajectories to Mount Wrangell in May 2004. The 10-day backward trajectories were analyzed using the trajectory model [Yamazaki, 1986] with 3D wind data from the GPV obtained from the JMA for May 2004. Each color denotes the air mass trajectory for a day. The denoted time is the start time of trajectory calculation in Coordinated Universal Time (UTC).

**Figure 6.** FD, CD, and tritium fluxes in each seasonal period. **(a)**: Early spring to late spring. **(b)** Late spring to summer. **(c)** Summer to fall. **(d)** Fall to winter. **(e)** Winter to early spring. Asterisks denote the data used for the correlation calculations (sample number: n). Also shown are the correlation coefficients between dust and tritium that had a significance level exceeding 90%.

**Figure 7.** Seasonal variations of tritium concentration from 1992–2002 in precipitation data at Anchorage station, which was obtained from IAEA-GNIP data [IAEA/WMO, 2004]. Error bars denote measurement errors.

**Figure 8.** Mass of calcium particles less than 2.5  $\mu\text{m}$  in diameter observed at Denali National Park; the data was supplied by the IMPROVE network. Bold line denotes 5-point running mean. Circles and diamonds with date denote the maxima of 5-point running mean corresponding to spring and other seasons, respectively.

**Figure 9.** Schematic of the annual relationship between Asian dust storm and the STE in late spring according to our proposal. If the Asian dust annually increases, the amount of STE will also increase.

Table 1: Correlation coefficients among the FD, CD, tritium fluxes and concentrations, and snow accumulation in each season



(a) From early spring to late spring (degree of freedom: n = 6)

	FD Flux	CD Flux	Tritium Flux	FD Con.	CD Con.	Tritium Con.	Snow Accum.
FD Flux	1.00	0.69	0.67	0.61	-0.03	0.39	0.69
CD Flux	0.69	1.00	0.30	0.58	0.58	-0.05	0.35
Tritium Flux	0.67	0.30	1.00	-0.14	-0.52	0.70	0.98
FD Con.	0.61	0.58	-0.14	1.00	0.54	-0.09	-0.14
CD Con.	-0.03	0.58	-0.52	0.54	1.00	-0.63	-0.48
Tritium Con.	0.39	-0.05	0.70	-0.09	-0.63	1.00	0.55
Snow Accum.	0.69	0.35	0.98	-0.14	-0.48	0.55	1.00

(b) From late spring to summer (degree of freedom: n = 7)

	FD Flux	CD Flux	Tritium Flux	FD Con.	CD Con.	Tritium Con.	Snow Accum.
FD Flux	1.00	0.70	0.78	0.69	0.08	0.29	0.77
CD Flux	0.70	1.00	0.47	0.41	0.64	0.04	0.55
Tritium Flux	0.78	0.47	1.00	0.19	-0.35	0.62	0.90
FD Con.	0.69	0.41	0.19	1.00	0.37	0.14	0.08
CD Con.	0.08	0.64	-0.35	0.37	1.00	-0.35	-0.26
Tritium Con.	0.29	0.04	0.62	0.14	-0.35	1.00	0.23
Snow Accum.	0.77	0.55	0.90	0.08	-0.26	0.23	1.00

(c) From summer to fall (degree of freedom: n = 4)

	FD Flux	CD Flux	Tritium Flux	FD Con.	CD Con.	Tritium Con.	Snow Accum.
FD Flux	1.00	0.56	0.41	0.54	-0.24	-0.21	0.81
CD Flux	0.56	1.00	0.17	-0.05	0.47	-0.31	0.73
Tritium Flux	0.41	0.17	1.00	0.19	-0.19	0.76	0.33
FD Con.	0.54	-0.05	0.19	1.00	0.02	0.08	-0.04
CD Con.	-0.24	0.47	-0.19	0.02	1.00	0.00	-0.25
Tritium Con.	-0.21	-0.31	0.76	0.08	0.00	1.00	-0.34
Snow Accum.	0.81	0.73	0.33	-0.04	-0.25	-0.34	1.00

(d) From fall to winter (degree of freedom: n = 5)

	FD Flux	CD Flux	Tritium Flux	FD Con.	CD Con.	Tritium Con.	Snow Accum.
FD Flux	1.00	0.65	0.46	0.81	0.45	0.27	0.65
CD Flux	0.65	1.00	0.66	0.69	0.95	0.69	0.23
Tritium Flux	0.46	0.66	1.00	0.19	0.51	0.95	0.52
FD Con.	0.81	0.69	0.19	1.00	0.67	0.15	0.09
CD Con.	0.45	0.95	0.51	0.67	1.00	0.63	-0.08
Tritium Con.	0.27	0.69	0.95	0.15	0.63	1.00	0.25
Snow Accum.	0.65	0.23	0.52	0.09	-0.08	0.25	1.00

(e) From winter to early spring (degree of freedom: n = 4)

	FD Flux	CD Flux	Tritium Flux	FD Con.	CD Con.	Tritium Con.	Snow Accum.
FD Flux	1.00	0.77	-0.36	0.91	0.75	-0.77	0.15
CD Flux	0.77	1.00	-0.67	0.78	0.99	-0.94	-0.05
Tritium Flux	-0.36	-0.67	1.00	-0.68	-0.74	0.53	0.74
FD Con.	0.91	0.78	-0.68	1.00	0.80	-0.69	-0.26
CD Con.	0.75	0.99	-0.74	0.80	1.00	-0.91	-0.15
Tritium Con.	-0.77	-0.94	0.53	-0.69	-0.91	1.00	-0.17
Snow Accum.	0.15	-0.05	0.74	-0.26	-0.15	-0.17	1.00

**Table 2.** Atmospheric Dust Concentration and Flux in Snow and Ice at Various Northern Hemisphere Sites<sup>a</sup>

	Site <sup>b</sup>		Elevation, m asl	Period, <sup>c</sup> (years AD)	Analytical Method <sup>d</sup>	Dust Concentration and Flux			Reference	
	Lat	Long				Size Range, $\mu\text{m}$	Number, $10^3 \text{ mL}^{-1}$	Mass, $\mu\text{g kg}^{-1}$		Flux, <sup>e</sup> $\mu\text{g cm}^{-2} \text{ yr}^{-1}$
Mount Wrangell (including Spurr)	62°N	144°W	4100	1992–2002	LLS	0.52–8	80.2	1511	84.7	this work
Mount Wrangell (excluding Spurr)							58.2	303	12.6	
Mount Wrangell WI–ES							70.7	498	20.3	
Mount Wrangell FA–WI							48.4	207	9.6	
Mount Wrangell SU–FA							151.6	6162	368.3	
Mount Wrangell SU–FA (excluding Spurr)							41.7	122	8.0	
Mount Wrangell LS–SU							51.7	228	13.1	
Mount Wrangell ES–LS							78.7	458	11.9	
Penny Ice Cap	67°N	65°W	1980	1988–1994	CC	0.65–12	31.6	143	4.8	Zdanowicz <i>et al.</i> [1998]
Agassiz Ice Cap	81°N	73°W	1600	1950–1977	CC	1–12	13.7	129	4.4	
				last 5000 years	CC	>1	18.3	na	na	Koerner and Fisher [1982]
Devon Ice Cap	77°N	82°W	1800	last 7000 years	CC	>1	18.2	na	na	Fisher and Koerner [1981]
					CC	>1	8.3	235	4.2	
Canada Basin	75°N	150°W	sea level	recent snow	FLTR	na	na	na	1.4–13.3	
Canada Basin	84°N	72°W	sea level	recent snow	FLTR	na	na	na	8.5–21	Darby <i>et al.</i> [1974]
Arctic Ocean (average)			sea level	recent snow	CHEM	na	na	na	3.1	Mullen <i>et al.</i> [1972] Rahn <i>et al.</i> [1979]
Summit Dye3	72°N	38°W	3207	recent snow	CC	0.5–12	na	46	1	Steffensen [1997]
	65°N	43°W	2479	last 10,000 years	LLS	0.2–4	na	50	2.5	Hammer <i>et al.</i> [1985]
				1978–1983	LLS	0.2–4	9.4	na	na	
				1780–1951	LLS	0.2–4	20.0	na	na	
Camp Century	77°N	61°W	1885	recent snow	CHEM	na	na	35	1.4	Murozumi <i>et al.</i> [1969]
				1753–1965	EM	0.02–8	na	35	1.4	Kumai [1977]
Sites A and D (average)	70°N	39°W	3070	1891–1910	LLS	0.2–4	na	74	2.5	Steffensen [1988]
Inland Sites (average)			>2400	1940–1950	LLS	>1	14	na	na	Hammer [1977]
Alaska Range (USA)	63°N	151°W	2500	recent snow	CHEM	na	na	300	na	Hinkley [1994]
Saint Elias Range (USA)	60°N	139°W	2600	recent snow	FLTR	na	na	na	16	Windom [1969]
Mount Olympus (USA)	47°N	123°W	2000	recent snow	FLTR	na	na	na	32	Windom [1969]
Mont Blanc (France)	45°N	6°E	4270	1955–1985	CHEM	na	na	na	21–35	De Angelis and Gaudichet [1991]
Colle Gnifetti (Switzerland)	46°N	7°E	4450	1936–1982	CC	0.63–16	37.0	na	na	Wagenbach and Geiss [1989]
Mustagh Ata (China)	38°N	75°W	5910	1990–1992	CHEM	na	na	na	20	Wake <i>et al.</i> [1994]
Ngozumpa Glacier (Nepal)	28°N	86°W	5700	1989–1990	CC	1–22	276.4	6780	247	Wake <i>et al.</i> [1994]
Chongce Ice Cap (China)	35°N	81°W	6327	1980–1987	CC	1–13	18.2	379	27	Wake <i>et al.</i> [1994]
					CC	1–22	616	8220	607	Wake <i>et al.</i> [1994]

<sup>a</sup>Modified from work by Zdanowicz *et al.* [1998] with permission from Zdanowicz *et al.* and Blackwell Publishing.

<sup>b</sup>Lat, latitude; Long, longitude.

<sup>c</sup>Period of snow accumulation represented by the data.

<sup>d</sup>Analytical methods: CC, Coulter counter or equivalent method; CHEM, calculated from chemical data (typically [Al], [Ca], or [Si]); EM, electron microscope; FLTR, based on dry filter weights; and LLS, laser light scattering.

<sup>e</sup>Flux values were taken from the literature or were calculated from mass concentrations using published estimates of snow accumulation rates. The units of seasonal Mount Wrangell Fluxes are  $\mu\text{g cm}^{-2} \text{ season}^{-1}$ .

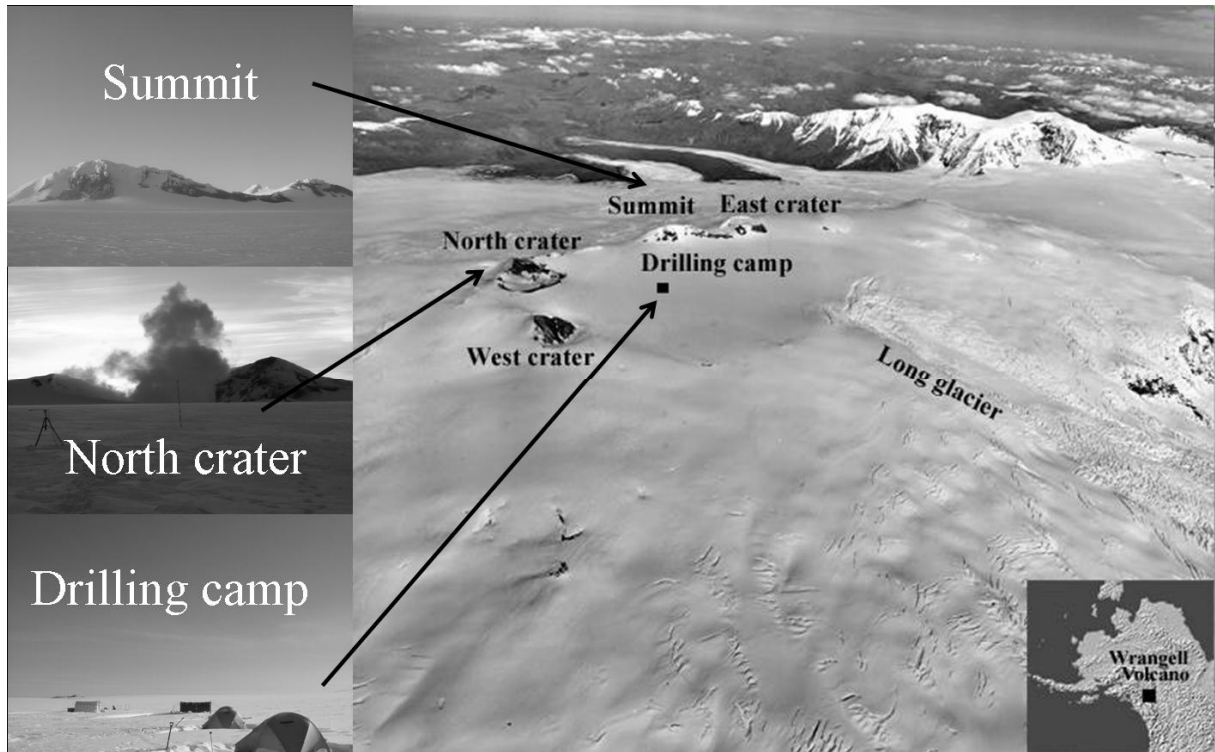


Figure 1.

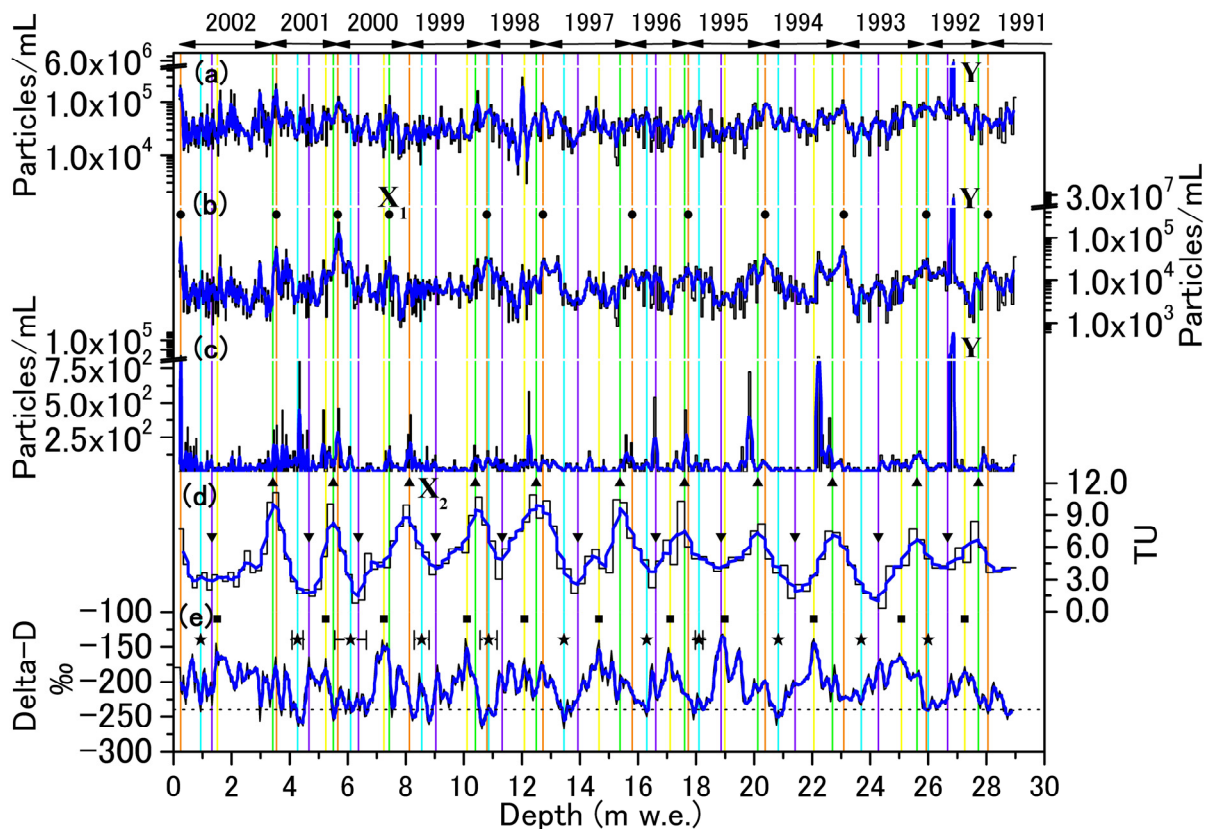
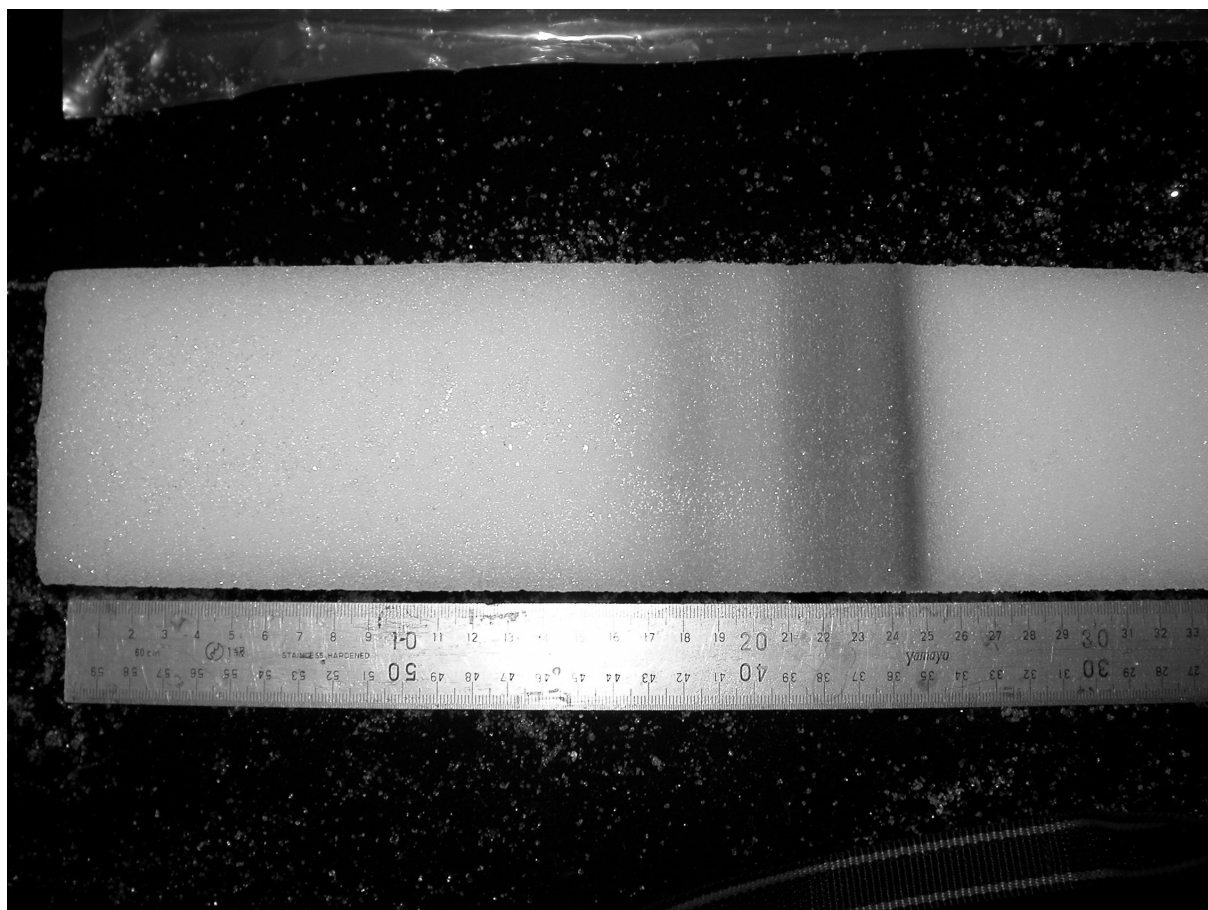


Figure 2.



**Figure 3**

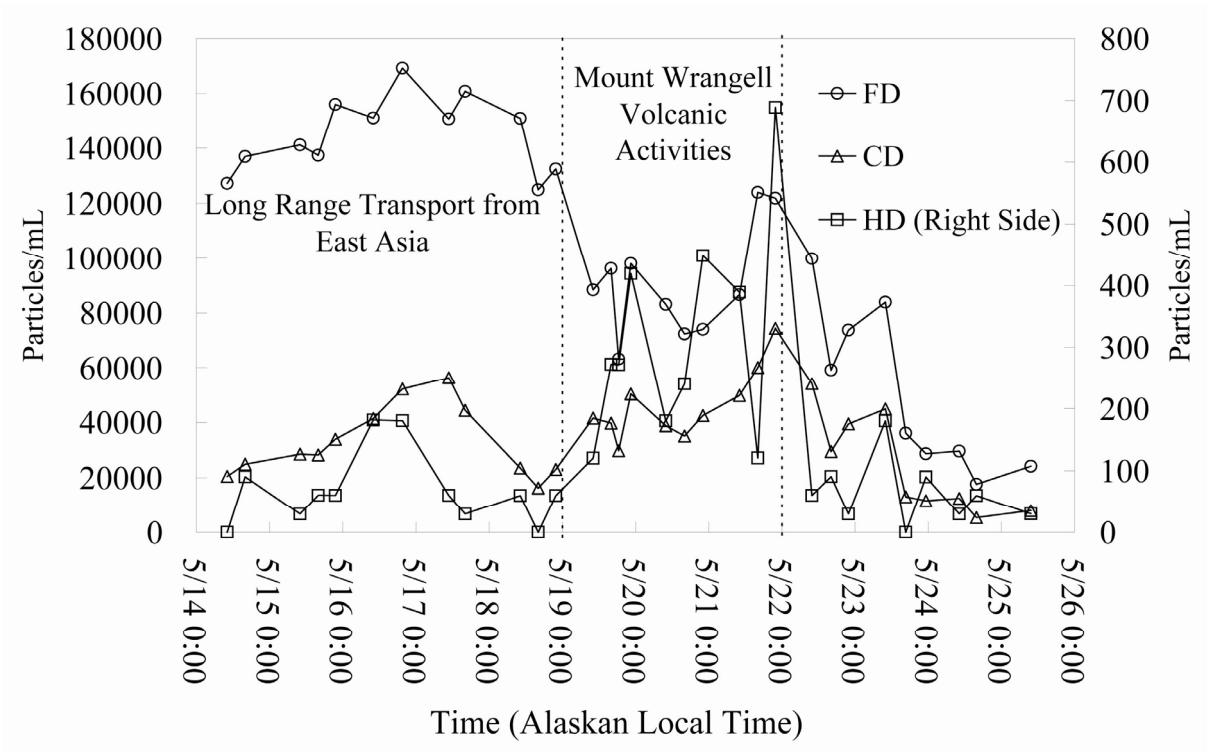
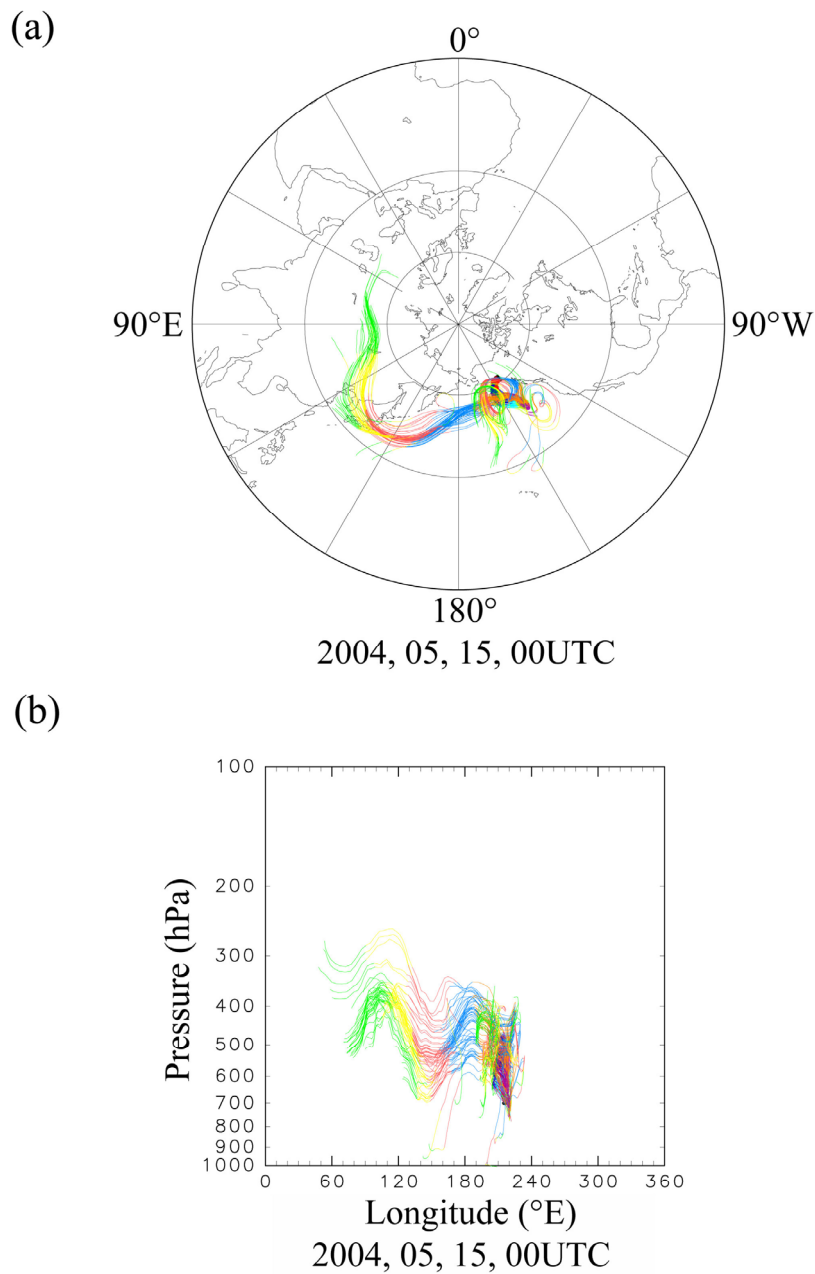


Figure 4.



**Figure 5.**

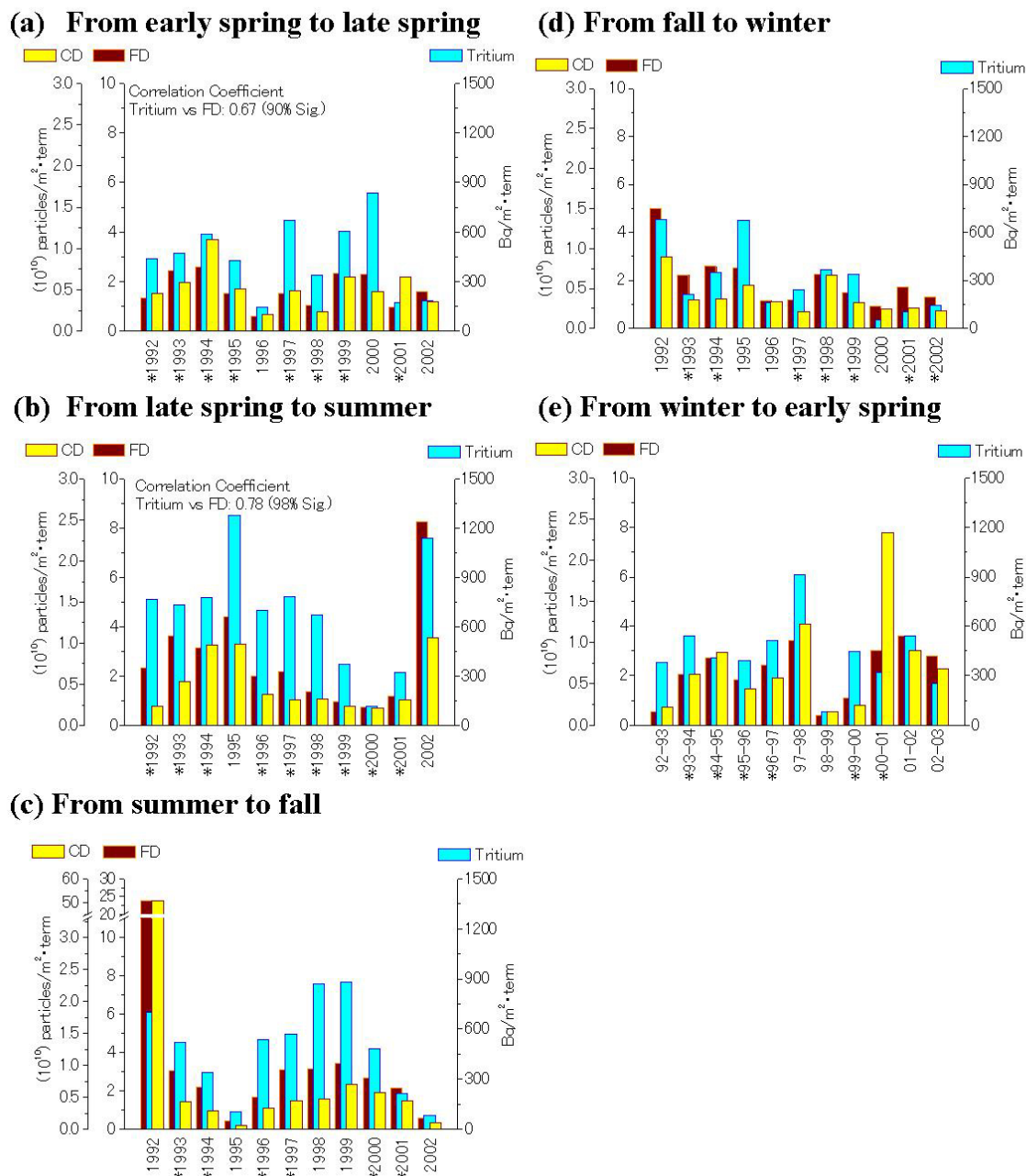


Figure 6.

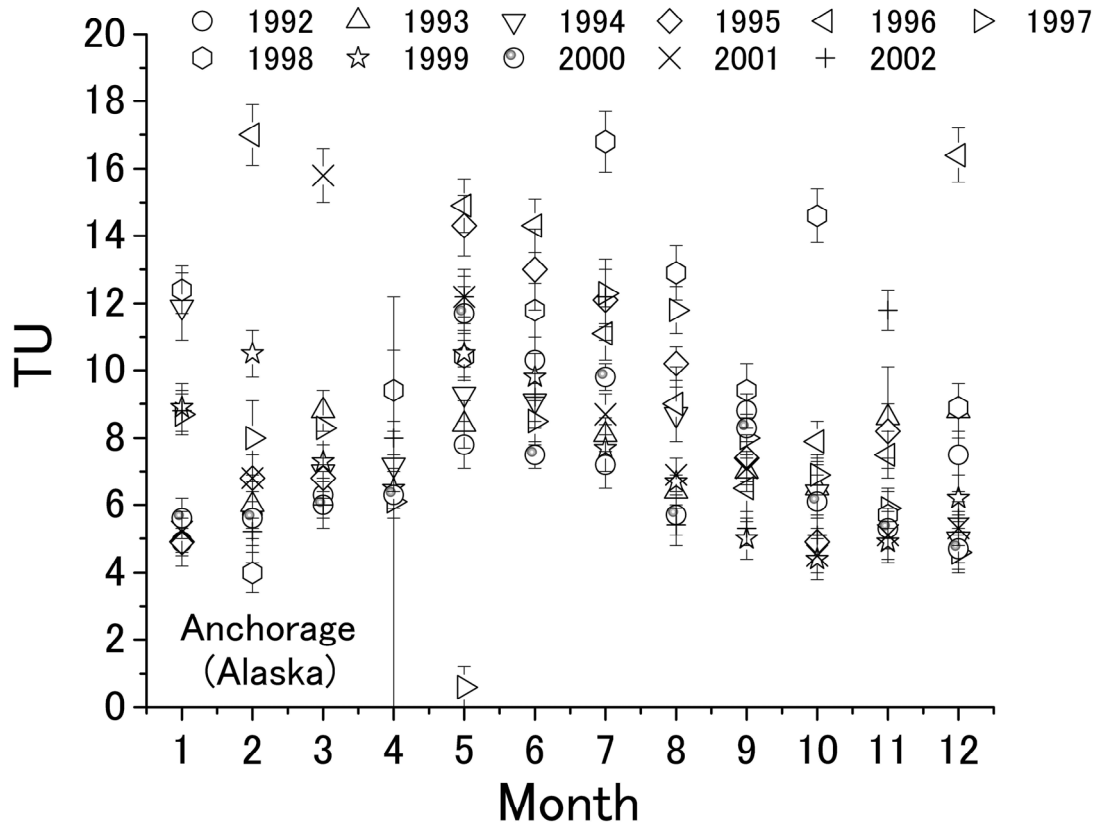


Figure 7.

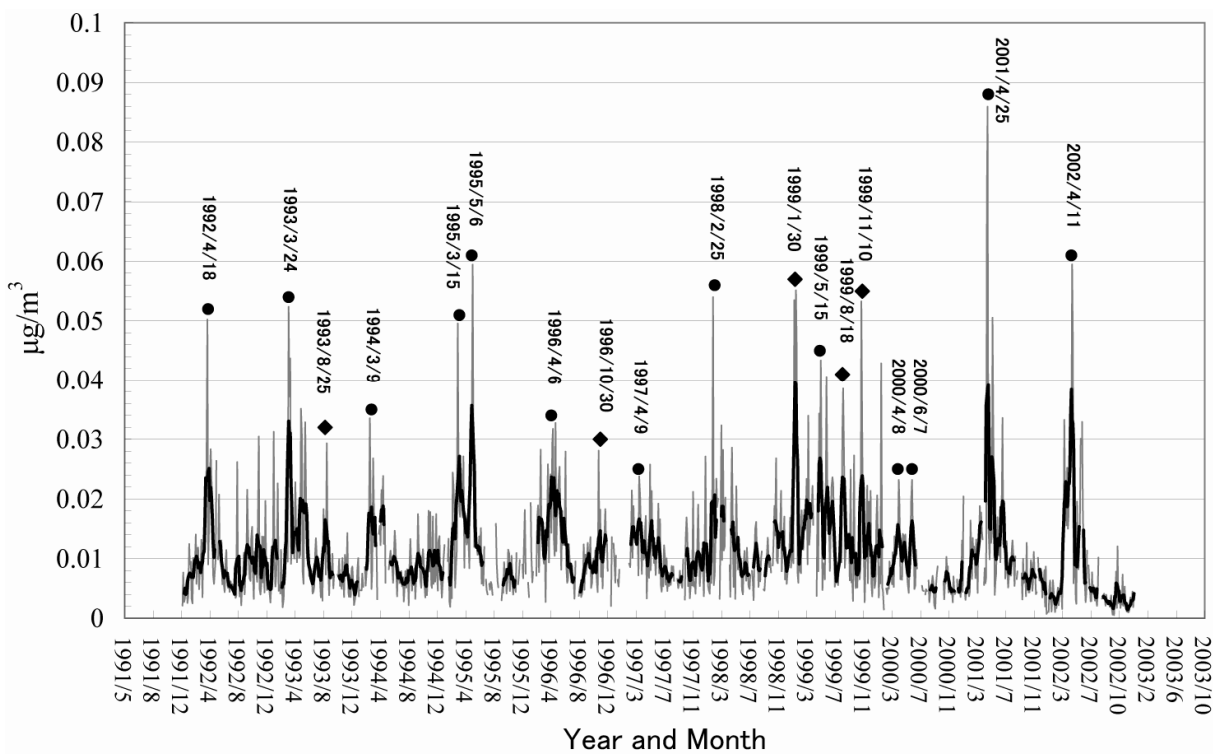


Figure 8.

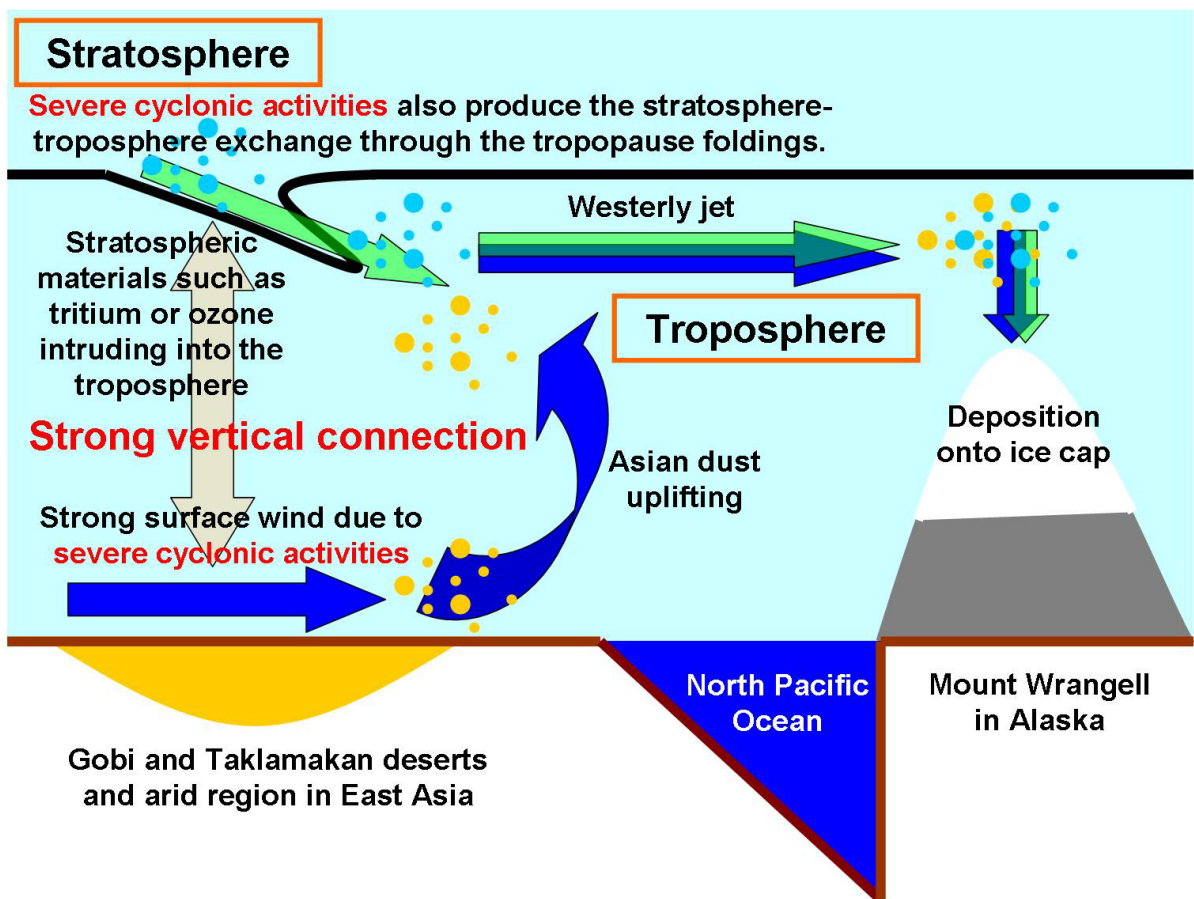


Figure 9.